ON THE NATURE OF THE $\gamma - \alpha$ PHASE TRANSITION IN CERIUM

G.Eliashberg[*+], H.Capellmann[+]

[+]Institut für Theoretische Physik , RWTH Aachen,
D-52056 Aachen, Germany

[*]Landau Institute for Theoretical Physics
142432 Chernogolovka, Russia

In 1964 Davis and Adams established that a large increase of thermal expansion and compressibility in the critical region of the γ- to α-Ce phase transition occurs predominantely in the α phase. This provides strong evidence that a tricritical point is realized in Ce. This also means that the above mentioned transition is not isomorphic and that α-Ce should have a distorted fcc structure. A scrupulous examination of Jayaraman's data (1965) shows that a second order transition line continues beyond the tricritical point to the vicinity of a triple point on the melting curve. The phase boundary with the tricritical point and the minimum of the melting curve are reconstructed within the framework of Landau theory.

PACS: 61.50.Ks, 81.30.-t

1. The $P - T$-phase diagram of Ce shows a multitude of phases. Except for the body-centered tetragonal phase appearing at room temperature above 120 kbar [1, 2] other known phases fall into a relatively low pressure domain. They are drawn in Fig. 1 which is to some extent schematic, reflecting a substantial experimental uncertainty. The data were taken from [2,3]. The line YZ is a second order transition boundary predicted in our paper. More precise data are available for the high-temperature part of Fig. 1, where the melting curve has a negative slope at ambient pressure and goes through a minimum at around 33 kbar and 935 K [4]. This remarkable feature will be discussed below. At the periphery of Fig. 1 one can see a body-centered cubic (bcc) δ-phase, a double-hexagonal close packed (dhcp) β-phase and two low symmetry phases α' (orthorhombic α-Uranium structure) and α'' (monoclinic body-centered) which at room temperature coexist in a fragile equilibrium for pressures between 40 and 120 kbar. The main part of Fig. 1 is occupied by the γ- and α-phases. The widely accepted view is that both γ-Ce and α-Ce have a simple face-centered cubic lattice. Across the line XY separating these phases a first order transition occurs. It was found that the volume and the entropy changes at the transition are large at room temperature and below $(\Delta v/v \gtrsim 15\%, \Delta s \gtrsim 1.5$ per atom) and tend to zero beyond 500 K, indicating the existence of a terminal point. Already in 1958 Ponyatovskii proposed that this might be a critical point like that in the vapour liquid system [5]. This implies a singular behaviour of the second derivatives of the thermodynamic potential (specific heat, compressibility, thermal expansion) which should tend to infinity at the critical point. Indeed in 1960 Beecroft and Swenson [6] observed a 10 fold increase of thermal expansion in a critical region with respect to that at ambient conditions. A few years later Davis and Adams [7] in their elegant X-ray diffraction study confirmed this effect, and this was considered as a further justification for the critical point concept. But they also made an additional observation, the importance of which was not properly taken account of: They were able to establish that a singular behavior

of thermal expansion and of compressibility occur only in the high pressure phase, that is in α-Ce. This was in fact an *experimentum crucis* which already long ago could have lead to the unambigous conclusion: instead of an ordinary critical point in Ce "the critical point of a continuous phase transition" is realized (the general concept was developed by Landau in 1935 - 37 [8, 9], and is now called a "the tricritical point"(proposed by Griffiths [10])). According to Landau a 1-st order phase transition between two phases having different symmetry continues beyond a tricritical point as a 2-nd order phase transition. In the vicinity of the tricritical point the compressibility etc. diverge, but only in that phase which has lower symmetry. This is exactly what was observed by Davis and Adams. We have to recognize therefore that α-Ce should have lower symmetry than γ-Ce. The phase transition from fcc to a distorted fcc-phase was also discovered in Lanthanum and in Praseodimium, the neighbours of Ce in the periodic table [11 – 14], and within this systematics a distorted fcc structure of α-Ce is quite reasonably expected. The diffraction patterns for the distorted structures in La and Pr show weak superlattice reflections together with the set of strong reflections typical for the fcc structure. Due to the topology of the phase diagram good long range ordered crystals of α-Ce have not been available, and substantial line broadening masks the weak superlattice reflections. In the past this prevented a direct observation of the distorted structure of α-Ce.
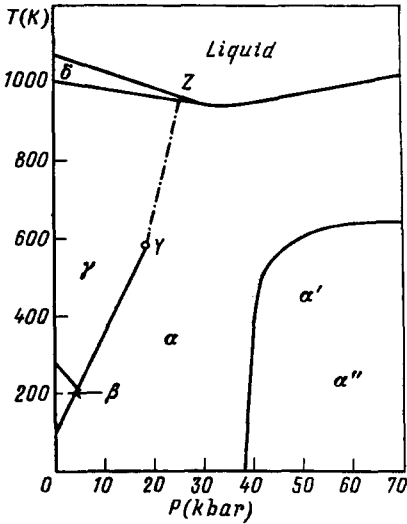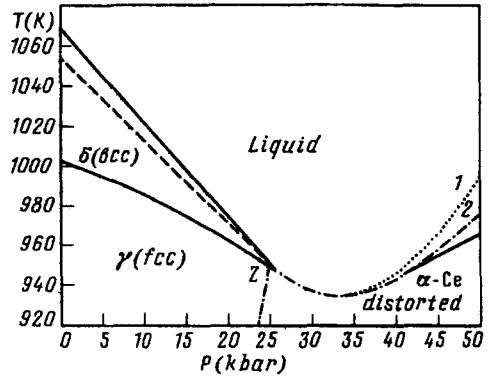

Fig.1   Fig.2.

2. In this section we analyse the experimental information regarding the high-temperature part of the phase diagram [4]. Clear evidence will be found for a second order $\gamma - \alpha$ transition in the vicinity of a triple point on the melting curve. In Fig. 2 the measured phase boundaries (solid lines) are shown together with our calculations (explained below). An important feature is the minimum of the melting temperature as a function of pressure. From the Clausius Clapeyron equation it follows that below the minimum ($P < 33$ kbar) the solid is less dense than the liquid, but the situation reverses at $P > 33$ kbar. Jayaraman [4] attributed this effect to a volume-pressure anomaly in the solid phase, supposing that liquid Ce is in a "collapsed state" already at ambient pressure showing the regular volume contraction along with increasing pressure. The anomaly in solid Ce, being very strong in the critical region around point Y should still be significant in the vicinity of the

melting curve. This explanation is no doubt qualitatively correct, but within the tricritical point scenario we have to take into account that the anomalous properties manifest themselves in the low-symmetry phase. This, therefore, has to be the α-phase, which exists in equilibrium with the liquid around the melting curve minimum. On the other hand it appears that the neighbouring phase below the border with the δ-phase is the high-symmetry phase, γ-Ce. This becomes apparent from the analysis of the corresponding boundary line, which we identify below as a $\gamma - \delta$-phase boundary. This line has a pronounced downward curvature (Fig. 2) and can be fitted by the equation

$$T = 1003 - 1.4P - 0.0305P^2 \qquad (1)$$

where T is in Kelvin and P in kilobar. The same equation we can write expanding the equilibrium condition for the chemical potentials ($\mu_\delta = \mu_\gamma$ at the boundary) in powers of P and $T - T_0, T_0 = 1003$ K:

$$-(s_\delta - s_\gamma)(T - T_0) + (v_\delta - v_\gamma)P - \frac{1}{2}(\kappa_\delta - \kappa_\gamma)P^2 = 0 \qquad (2)$$

Here s is the entropy per atom, v - the atomic volume and $\kappa = -dv/dP$ is the compressibility. Other quadratic terms which are due to the thermal expansion and the heat capacity differences give negligible contributions. From the measured data we calculate the volume and entropy changes across the transition at $P = 0$:

$$v_\delta - v_\gamma = -0.062\text{Å}^3 \; ; \; s_\delta - s_\gamma = 0.044\text{Å}^3\text{kbar/K} \qquad (3)$$

($1\text{Å}^3\text{kbar/K}$ corresponds to the dimensionless value 7.25 for the entropy per atom). Comparing eqs. (1) and (2) we find the compressibility difference

$$\kappa_\delta - \kappa_\gamma \simeq 0.0027\text{Å}^3/\text{kbar} \qquad (4)$$

which is only $\sim 2\%$ of κ_γ($\kappa_\gamma \approx 0.15\text{Å}^3/\text{kbar}$ for the bulk modulus $K \approx 230$ kbar and $v_\gamma \approx 34\text{Å}^3/\text{kbar}$): There is no evidence for any anomalous increase of κ_γ. This means that Ce indeed remains in its "normal" high-symmetry γ-phase along most of the $\gamma - \delta$ line. We come to the conclusion that a possible position of point Z is limited to an interval of a few kilobar around the triple point (see Fig. 2) being either on the $\gamma - \delta$ line or on the melting curve.

We can now calculate the coordinates of point $Z, (P_Z, T_Z)$, and the compressibility jump at the $\gamma - \alpha$ transition. Suppose first that $P_Z > 26$ kbar. Beyond Z the liquid is therefore in equilibirum with the α-phase: $\mu_{liq} = \mu_\alpha, \mu_\alpha = \mu_\gamma + \Delta\mu$. Expanding $\mu_{liq} - \mu_\gamma$ in powers of $P - P_Z$ and $T - T_Z$ we get the equation for the melting curve, $P > P_Z$:

$$-(s_{liq} - s_\gamma)(T - T_Z) + (v_{liq} - v_\gamma)(P - P_Z) - \frac{1}{2}(\kappa_{liq} - \kappa_\gamma)(P - P_Z)^2 - \Delta\mu = 0 \qquad (5)$$

The main contribution to $\Delta\mu$ is due to the compressibility jump $\Delta\kappa$:

$$\Delta\mu = -\frac{1}{2}\Delta\kappa \cdot (P - P_Z)^2. \qquad (6)$$

From the linearity of the border between the liquid and the δ-phase we find that $\kappa_{liq} = \kappa_\delta$ and therefore $\kappa_{liq} - \kappa_\gamma = \kappa_\delta - \kappa_\gamma$, Eq.(3). Using the measured data we also get

$$v_{liq} - v_\delta = -0.38 \; ; \; s_{liq} - s_\delta = 0.081 \qquad (7)$$

(the units are as in Eq. (3)).

These values remain constant along the melting line. According to Eqs. (3) and (4) $v_\delta - v_\gamma = -0.13$ at the triple point, while $s_\delta - s_\gamma$ does not change appreciably. Using the values of Eq. (6) we get finally the coefficients in Eq. (5):

$$v_{liq} - v_\gamma = -0.51 \; ; \; s_{liq} - s_\gamma = 0.125. \tag{8}$$

The initial slope of the melting curve on the high pressure side of the triple point is therefore equal to 4.1 K/kbar. Defining a straight line having this slope and going through the triple point (dashed line in Fig. 2)

$$T = 1053 - 4.1P, \tag{9}$$

we impose three conditions, necessary to calculate T_Z, P_Z and $\Delta\kappa$: T_Z and P_Z satisfy Eq. (9); the coordinates of the melting curve minimum, $T_m = 935$ K and $P_m = 33$ kbar, satisfy Eq. (5), and $dT/dP = 0$ at the minimum of the melting curve Eq.(5). Solving the corresponding equations we find that

$$\Delta\kappa \approx 0.065 \text{Å}^3/\text{kbar} \tag{10}$$

and $P_Z \approx 25$ kbar. This value is indeed very close to (but $\sim$ 1 kbar below) the triple point. As a result, the calculated point is not the true point Z, but point Z' which falls on the line Eq.(9) at a temperature $T_Z' \simeq 951$ K about 4 K above the $\gamma-\delta$-phase boundary. The estimations show that with the accuracy of $\sim$ 1 K and a few tenth of kilobar we can simply take the projection of Z' on the $\gamma - \delta$-line to get a correct position of point Z:

$$P_Z \approx 25 \text{ kbar} , \; T_Z \approx 947 \text{ K}. \tag{11}$$

The melting curve calculated using the Eqs. (5) and (6) (with T_Z' instead of T_Z!) and shown as curve 1 in Fig. 2. coincides with the measured one along an interval of about 10 kbar beyond the triple point.

The discrepancy at higher pressure is, of course, not surprising for an approximate version of $\delta\mu$, Eq. (6), and is diminished within a more general description (curve 2 on Fig. 2; see next section).

3. It is most natural to expect that a second order transition line continues from point Z to the tricritical point Y. Beyond Y a wellknown first order phase transition occurs (Fig. 1), and to get a quantitative description of this peculiar situation we expand (following Landau [8, 9]) the chemical potential $\mu(P,T,u) = \mu(P,T,0) + \Delta\mu(P,T,u)$ in powers of some amplitude u, related to the lattice distortion:

$$\Delta\mu = Au^2 + Bu^4 + Cu^6 , \; C > 0. \tag{12}$$

To avoid misunderstanding we note that the transition to the distorted structure is, most probably, driven by the softening of some phonon mode at a high-symmetry point in the Brillouin zone (see Sec. 4). The resulting distortion is some definite superposition of displacements (corresponding to several points with the same symmetry) which provides the minimum value of the 4-th order term. The expansion Eq. (12) is written for the amplitude u of this already selected superposition.

At $B(P,T) > 0$ a second order transition occurs along the line ZY, defined by the equation $A(P,T) = 0$; $A > 0, u = 0$ for a "normal" γ-phase, $A < 0, u \neq 0$ for a distorted α-phase. Let $(P'T')$ be some point on ZY. Using the expansion

$$A(P,T) = \alpha(P'T')(T - T') - \beta(P'T')(P - P') \tag{13}$$

114

we find the discontinuities of the compressibility $\kappa = -dv/dP$, the thermal expansion $\eta = dv/dT$ and the heat capacity c (per atom):

$$\Delta\kappa = \frac{\beta^2}{2B} \ , \ \Delta\eta = \frac{\alpha\beta}{2B} \ , \ \Delta c = T'\frac{\alpha\beta}{2B} \tag{14}$$

where $\Delta\kappa = \kappa_\alpha - \kappa_\gamma$ etc., and all quantities depend on P', T'.

The tricritical point Y appears as a crossing point of lines $A(P,T) = 0$ and $B(P,T) = 0$. In the vicinity of Y

$$B(P,T) \approx B_0(P,T) = \gamma(T - T_Y) - \beta(P - P_Y) \tag{15}$$

and $\Delta\kappa, \Delta\eta, \Delta c$ tend therefore to infinity as $(T' - T_Y)^{-1}$.

Below T_Y the $\gamma - \alpha$ phase bondary continues as a line of first order transitions: $B^2 = 4AC$ [9]. Within the scope of Eq. (13), taken around Y, and Eq. (16) the phase boundary is defined by a simple quadratic equation. In terms of the dimensionless variables t and p

$$t = \frac{T - T_Y}{T_Z - T_Y} \ , \ p = \frac{1}{P_0}\left(P - P_Y - \frac{T - T_Y}{k_A}\right) \tag{16}$$

this equation is (for $t < 0$):

$$p + \frac{3}{4}(t - \nu p)^2 = 0 \ , \ \nu = \frac{k_A k_B}{k_A - k_B}\frac{P_0}{T_Z - T_Y}, \tag{17}$$

where

$$P_0 = \frac{B_0^2(Z)}{3\beta C} \ , \ k_A = \frac{\beta}{\alpha} \ , \ k_B = \frac{\delta}{\gamma} \tag{18}$$

and $B_0(Z) = \gamma(1 - k_B/k_A)(T_Z - T_Y); \alpha = \alpha(Y), \beta = \beta(Y)$ (see Eq. (13)). Although the information concerning the position of the singular-point Y is vague, the measured temperature evolution of the pressure-resistance isotherms [4] shows that 530 - 560 K is the most plausible interval for T_Y. Taking $T_Y = 550$ K and $k_A = (T_Z - T_Y)/(P_Z - P_Y)$ (supposing ZY is close to a straight line) we have calculated P_Y and the parameters P_0 and ν, fitting Eq.(17) to the measured characteristics of the phase boundary. For the values

$$P_Y = 16.7 \text{ kbar}, \quad P_0 = 28 \text{ kbar} \ , \ \nu = 1.12 \tag{19}$$

the theoretical curve

$$p(t) = -\frac{2}{3\nu^2}(1 - \frac{3}{2}\nu t - \sqrt{1 - 3\nu t}), \quad t < 0 \tag{20}$$

goes through the point $P = 7.2$ kbar at $T = 300$ K and is nearly linear up to 450 K, having a slope $k(T) = dT/dP$ slowly changing from 22 to 27 K/kbar. These characteristics reproduce the measured data well within the experimental uncertainties. Above 450 K $k(T)$ increases to the value $k_A \approx 48$ K/kbar at point Y. A substantial increase of $k(T)$ above 450 K was reported [15] but, in total, the data in this region are controversal.

Provided $\Delta\mu$, Eq. (13), is minimal [9], u^2 in terms of p, t is defnded by the equation:

$$\beta u^2 = 2P_0(\Delta\kappa)_0 f \ ; \quad (\Delta\kappa)_0 = \beta^2/2B_0(Z), \tag{21}$$

where

$$f = f(t,p) = -t + \nu p + \sqrt{(t - \nu p)^2 + p}. \tag{22}$$

Inserting Eq.(22) into Eq.(13) we get $\Delta\mu(p,t)$:

$$\Delta\mu = -\frac{2}{3}(\Delta\kappa)_0 P_0^2 [2p - (t - \nu p)f]f \tag{23}$$

and for $\Delta v = \partial\Delta\mu/\partial P$ and $\Delta s = -\partial\Delta\mu/\partial T$ we find:

$$\Delta v = -2(\Delta\kappa)_0 P_0 (1 + \nu f)f \; ; \; \Delta s = -2(\Delta\kappa)_0 P_0 \left(\frac{1}{k_A} + \frac{\nu}{k_B}f\right)f \; . \tag{24}$$

In particular, at the first order transition line Eq. (20), $t < 0$,

$$f(t, p(t)) = \frac{1}{\nu}(\sqrt{1 + 3\nu|t|} - 1) \tag{25}$$

and using the measured value of the volume jump at $T = 300\,\text{K}$, $\Delta v \approx 4.5 \div 4.8\,\text{Å}^3$ [3] we find (for P_0, ν Eq. (19)):

$$(\Delta\kappa)_0 \approx 0.067 \div 0.072 \; \text{Å}^3/\text{kbar}. \tag{26}$$

Using $k_A = 48\,\text{K/kbar}$ and $k_B = 12\,\text{K/kbar}$ (for $\nu = 1.12$, Eq.(17)), we find from Eq. (24): $\Delta s = -(1.61 \div 1.73)$ per atom, $T = 300\,\text{K}$, in agreement with the measured value [3].

We emphasize that $(\Delta\kappa)_0$ in Eq. (26) is close to $\Delta\kappa$ in Eq. (10). Comparing Eq. (14) for $\Delta\kappa$ and Eq. (21) for $(\Delta\kappa)_0$ we see that the similarity obtained is consistent with the characteristic temperature scale in the expansion of B, Eq. (15), being much larger than $T_Z - T_Y$ and with $\alpha(P'T')$ and $\beta(P'T')$, Eq. (13), only weakly changing along the ZY-line. This does not seem surprising: within the considered interval T is several times the Debye temperature $\Theta \approx 130\,\text{K}$ and the scale mentioned above should be of electronic origin.

The line $A(P, T) = 0$, which is confined to a relatively narrow pressure interval ($P_Z - P_Y \approx 8\,\text{kbar}$), is therefore close to a straight line (as was supposed above.). Another basic line, $B(P, T) = 0$, having a much smaller slope continues to the higher pressure region. On a very qualitative ground one can expect the bulk modulus ($\sim 200\,\text{kbar}$) to be an appropriate pressure scale in the expansion of B, Eq. (15), but because a linear term is relatively small ($k_B \approx 0.25 k_A$ at $P = P_Y$), the nonlinear dependence on P may become important at much lower pressure. Indeed, inserting $\Delta\mu$, eq. (23), into eq.(5) for the melting curve, we found (for the calcualted values of parameters) a substantial deviation from the measured curve already at $P \sim 33\,\text{kbar}$. We therefore take into account the quadratic term $\sim (P - P_Y)^2$ in Eq. (15):

$$B(P, T) \approx \gamma \left[T - T_Y - k_B(P - P_Y)\left(1 - \frac{P - P_Y}{Q}\right)\right]. \tag{27}$$

Performing corresponding changes in $\Delta\mu$ we got a reasonably good fit of the melting curve for $Q = 40\,\text{kbar}$ (curve 2 in Fig. 2). As is seen, for this Q, a line $B(P, T) = 0$, having a slope $k_B = 12\,\text{K/kbar}$ at $P = P_Y(\approx 17\,\text{kbar})$, appraoches a maximal $T = 670\,\text{K}$ at $P = 37\,\text{kbar}$. Within this model only small (5 - 10%) corrections to the above determined parameters, P_0, ν and $\Delta\kappa$, are required to keep an equally good quantitative description simultaneously in both domains of the phase diagram, where reliable data are available: around the melting curve minimum and at $T < T_Y$ where the first order transition occurs.

4. The coefficient β in Eq. (21) for u^2 does not enter explicitly in $\Delta\mu$, Eq.(23), and to determine β, microscopic information has to be involved. In La and Pr the observed distortion of the fcc lattice is related to the softening of the zone-boundary transverse mode (so-called point L in the Brillouin zone) [11, 13]. The dispersion anomalies of this mode and the frequencies $\omega(L)$, measured in Ce [16] and in La [17, 18], are almost identical and one can expect in both metals the same mechanism driving the lattice distortion. Supposing this is the case, we can estimate β using a value of $\omega(L)$, measured at $P = = 0$. Extrapolating Eq. (13) (for $P' = P_Y, T' = T_Y$) to $P = 0$ we have in harmonic approximation: $A = \beta P_Y = M\omega^2/2$ (M - atomic mass). An appreciable softening of the transverse L-mode in Ce was observed from $T \sim 900\,\text{K}$ to room temperature [18]. We take roughly $\omega = 2\pi \cdot 10^{12}\text{sec}^{-1}$ for $T = T_Y$. We get (for $P_Y \approx 17\,\text{kbar}$) : $\beta \approx 30\,\text{Å}$ and

$$u^2 = \ell_0^2 f(p,t) \,, \ \ell_0^2 = \frac{2P_o(\Delta\kappa)_0}{\beta} \approx 0.1\text{Å}^2 \,, \tag{28}$$

which is comparable with the displacements measured in Pr [13].

It is worth pointing out, that the above mentioned instability results in a distorted lattice having at least two nonequivalent atomic positions in the unit cell. Each atom is displaced, therefore, from the centrally symmetric position, showing that an ionic core polarization is the source for the lattice instability. Followed by a mixing of electronic orbitals (having different local parity) this polarization gives rise to the softening of the phonon modes and to a strong modification of the electronic properties.

1. J.Staun Olsen, L.Gerward, U.Benedict and J.-P.Itié, Physica **133 B**, 129 (1985).
2. Y.C.Zhao and W.B.Holzapfel, J. of Alloys and Compounds **246**, 216 (1997).
3. D.A.Koskenmaki and K.A.Gschneidner, Jr., in: *Handbook on the Physics and Chemistry of Rare Earth*, Eds. K.A.Gschneidner, Jr. and L.Eyring North-Holland, Amsterdam, 1978, Chap. 4.
4. A.Jayaraman, Phys. Rev. **137A**, 179 (1965).
5. Ye.G.Ponyatovskii, Dokl. Akad. Nauk SSSR **120**, 10221 (195).
6. R.I.Beecroft and S.A.Swenson, J. Phys. Chem. Solids **15**, 234 (1960).
7. B.L.Davis and L.H.Adams, J. Phys. Chem. Solids **25**, 379 (1964).
8. L.D.Landau, Phys. Z. Sowjet **8**, 113 (1935); ibid. **11**, 26 (1937).
9. L.D.Landau and E.M.Lifshitz, *Course of Theoretical Physics*, vol. 5, Statistical Physics, Pergamon Press, Oxford 1958.
10. R.B.Griffiths, Phys. Rev. Lett. **24**, 715 (1970).
11. W.A.Grosshans, Y.K.Vohra, and W.B.Holzapfel, Phys. Rev. Lett. **49**, 1572 (1982).
12. F.Porsch and W.B.Holzapfel, Phys. Rev. Lett. **70**, 4087 (1993).
13. N.Hamaya, Y.Kakamoto, H.Fujihisa et al., J. Phys.: Condens. Matter **5**, L369 (1993).
14. Y.C.Zhao, F.Porsch, and W.B.Holzapfel, Phys. Rev. **B52**, 134 (1995).
15. L.D.Livshitz, Yu.S.Genshaft, and V.K.Markof, ZhETF **43**, 1262 (1962) (Sov. Phys. JETP **16**, 894 (1963)).
16. C.Stassis, T.Gould, O.D.McMasters et al., Phys. Rev. **B19**, 5746 (1979).
17. C.Stassis, C.-K.Loong, and J.Zaretsky, Phys. Rev. **B26**, 5426 (1982).
18. C.Stassis, G.Smith, B.N.Harmon et al., Phys. Rev. **B31**, 6298 (1985).
19. C.Stassis, C.-K.Loong, G.D.MacMasters, and R.M.Nicklow, Phys. Rev. **B25**, 6485 (1982).